TMPM Tschermaks Min Petr Mitt (1986) 35: 167–192

TMPM Tschermaks Mineralogische und Petrographische Mitteilungen

From the Institut für Angewandte Geophysik, Petrologie und Lagerstättenforschung, Technische Universität Berlin, the Lehrstuhl für Angewandte Mineralogie und Geochemie, Technische Universität München, Garching, Federal Republic of Germany, and the Institut für Mineralogie der Universität Kiel, Kiel, Federal Republic of Germany

Rock Forming Beryl from a Regional Metamorphic Terrain (Tauern Window, Austria): Parageneses and Crystal Chemistry

G. Franz, G. Grundmann, and **D. Ackermand**

With 11 Figures

Received October 3, 1985;
accepted May 15, 1986

Summary

Beryls from three localities (Felbertal, Habachtal and Schrammacher) in metamorphic rocks of similar metamorphic grade from the Tauern Window, Austria, were analyzed by electron microprobe. The results show that beside the main elements, Na, Mg, and Fe are important constituents. The most probable substitutions are

$$Al^{VI} + \square^{channel} = Mg^{VI} + Na^{channel}$$
$$Al^{VI} + \square^{channel} = Fe^{2+,VI} + Na^{channel}$$
$$Al^{VI} = Fe^{3+,VI}$$

Fe is present in both valence states, as Fe^{2+} and Fe^{3+}. Each occurrence of beryl has its typical $Mg/(Fe_{tot} + Mg)$ ratio reflecting the bulk chemistry of the host rock. Most of the beryls are chemically zoned with decreasing Al- and increasing $(Na+Mg+Fe_{tot})$-contents towards the margin. The zoning is described as an exchange reaction with coexisting sheet silicates (mica or chlorite) and albite.

Coexisting minerals with beryl are quartz, plagioclase, K-feldspar, biotite, muscovite, margarite, chlorite, talc, amphibole, epidote, garnet, phenakite, calcite, fluorite (+ accessory phases).

The $Mg/(Mg + Fe^{2+}_{tot})$ ratio varies in the order
beryl $\simeq$ talc $\geqslant$ actinolite $>$ biotite $\simeq$ chlorite $>$ phengite (Habachtal)
beryl $>$ phengite $>$ biotite $>$ garnet (Schrammacher)
phengite $\geqslant$ beryl $\geqslant$ biotite (Felbertal).

Textural relations show that the beryls grew after the main deformation of the rocks and that in many cases phenakite is transformed into beryl by the reactions

(1) 3 phenakite + 2 muscovite + 9 quartz = 2 beryl + 2 K-feldspar + H_2O
(2) 3 phenakite + 5 muscovite + chlorite = 2 beryl + 5 biotite + 2 quartz + 6 H_2O
(3) 3 phenakite + 9 quartz + 4 $Al(OH)_3$ *aq* = 2 beryl + 4 H_2O

It is concluded that both, bulk rock chemistry and composition of the fluid phase determine the composition of beryl.

Zusammenfassung

Beryll als gesteinsbildendes Mineral aus einem regionalmetamorphen Gebiet (Tauernfenster, Österreich)

Beryll von drei Vorkommen (Felbertal, Habachtal und Schrammacher) in Metamorphiten ähnlichen Metamorphosegrades aus dem Tauernfenster, Österreich, wurden mit der Elektronenstrahlmikrosonde untersucht. Die Ergebnisse zeigen, daß außer den Hauptelementen die Elemente Na, Mg und Fe wichtige Bestandteile sind. Die wahrscheinlichsten Substitutionen sind

$$Al^{VI} + \square^{Kanal} = Mg^{VI} + Na^{Kanal}$$
$$Al^{VI} + \square^{Kanal} = Fe^{2+,VI} + Na^{Kanal}$$
$$Al^{VI} = Fe^{3+,VI}$$

Fe ist sowohl als Fe^{2+} als auch als Fe^{3+} vorhanden. Jedes Beryllvorkommen ist durch ein typisches $Mg/(Fe_{tot} + Mg)$-Verhältnis charakterisiert, abhängig von der Gesamtzusammensetzung des Gesteins. Die meisten Berylle sind zonar gebaut mit abnehmendem Al- und zunehmenden $(Na+Mg+Fe_{tot})$-Gehalten zum Rand hin. Der Zonarbau wird als Austauschreaktion mit koexistierenden Schichtsilikaten (Glimmer oder Chlorit) und Albit beschrieben.

Mit Beryll koexistierende Minerale sind Quarz, Plagioklas, K-Feldspat, Biotit, Muskovit, Margarit, Chlorit, Talk, Amphibol, Epidot, Granat, Phenakit, Calcit, Fluorit (+ Akzessorien).

Das $Mg/(Fe_{tot} + Mg)$-Verhältnis ändert sich in der Reihenfolge
Beryll $\simeq$ Talk $\geqslant$ Aktinolith $>$ Biotit $\simeq$ Chlorit $>$ Phengit (Habachtal)
Beryll $>$ Phengit $>$ Biotit $>$ Granat (Schrammacher)
Phengit $\geqslant$ Beryll $\geqslant$ Biotit (Felbertal)

Die Texturen zeigen, daß Beryll nach der Hauptdeformation der Gesteine sproßte und daß in vielen Fällen Phenakit in Beryll umgewandelt wurde durch die Reaktionen

(1) 3 Phenakit + 2 Muskovit + 9 Quartz = 2 Beryll + 2 K-Feldspat + H_2O
(2) 3 Phenakit + 5 Muskovit + Chlorit = 2 Beryll + 5 Biotit + 2 Quartz + 6 H_2O
(3) 3 Phenakit + 9 Quarz + 4 $Al(OH)_3$ *aq* = 2 Beryll + 4 H_2O

Sowohl der Gesamtgesteinschemismus als auch die Zusammensetzung der fluiden Phase bestimmen die Zusammensetzung des Berylls.

Introduction

Beryl is an accessory mineral in many granitic rocks; for a review of the crystal chemistry and the mode of formation of beryl in these rocks see Beus (1966). Relatively little is known about beryls from other geological settings such as alpine fissures (Hänni 1980), about emerald (Franz 1982), in many cases of hydrothermal or pegmatitic origin (Sinkankas 1981) and about beryl as a constituent of regional metamorphic rocks in alpine type orogenic areas.

Within the Central and Western Tauern Window (Austria), an area strongly influenced by Alpine regional metamorphism, three different occurrences of rock forming beryl are known: Felbertal, Habachtal and Schrammacher. The aim of this paper is to study the crystal chemistry of beryl including chemical zonation together with the crystal chemistry of accompanying minerals. This work allows us to derive possible mechanism of substitution that are operative in beryl, to describe the variation in major elements, and to discuss the mineral forming process in these regional metamorphic rocks.

Fig. 1 shows the geological setting of the three investigated occurrences Felbertal (F), Habachtal (H), and Schrammacher (S) on a simplified geological

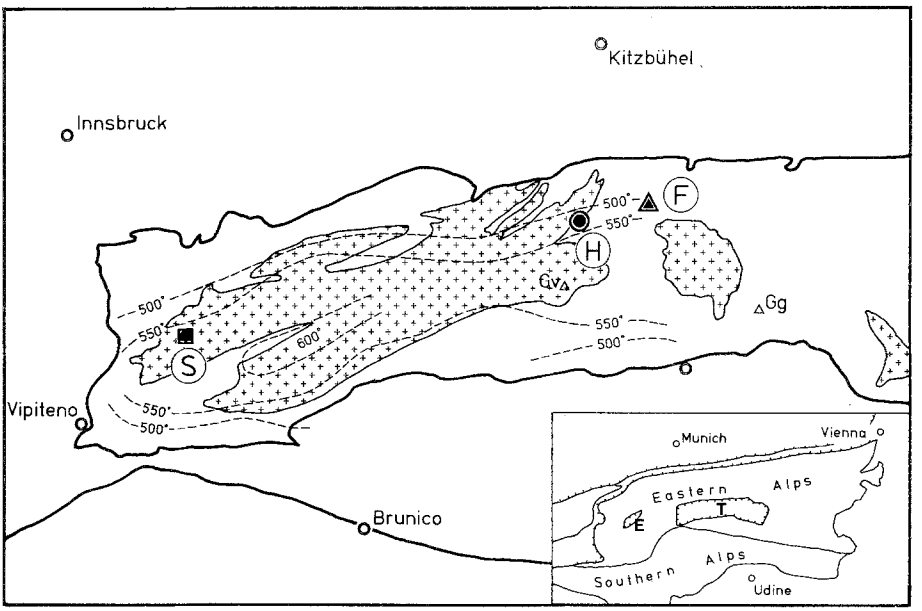

Fig. 1. Sample localities S = Schrammacher, H = Habachtal, and F = Felbertal within the Tauern Window (outlined; crosses = central gneiss cores, blank = Schieferhülle series). Dashed lines indicate oxygen isotope equilibrium temperatures for the alpine regional metamorphism according to Hoernes and Friedrichsen (1976). Inset shows the tectonic position of the Tauern Window (= T) in the Eastern Alps

map of the Tauern area. All three occurrences are situated within the Venediger nappe (Frisch 1977), the deepest tectonic unit of the Pennine domain in the Eastern Alps. The Venediger nappe is subdivided into two tectonolithological units, the central gneiss core (Zentralgneiskern) and the lower schist cover (Untere Schieferhülle) (Morteani 1974). Two of the beryl occurrences are situated within the lower schist cover (Felbertal and Habachtal), and the third one (Schrammacher) lies within the central gneiss core. The most important geological features are summarized in Table 1. Both, the Habachtal and the Felbertal are polymetamorphic and have experienced the hercynian as well as the alpine orogeny (Grundmann and Morteani 1982); it is not clear, however, whether or not the Schrammacher gneiss core was influenced by the hercynian metamorphism (for a detailed discussion of this problem see Satir and Morteani 1982).

The temperatures of alpine metamorphism according to oxygen isotopic data (Hoernes and Friedrichsen 1974) are in the same order of magnitude for all three localities, i.e. 500–550 °C, though somewhat higher for the Schrammacher (~ 550 °C). Pressures represent in all cases the conditions of a late equilibration. Selverstone et al. (1984) recognized an earlier high pressure metamorphism in the Greiner Series of the Tauern Window, and there are some indications that earlier pressures in other units of the Tauern were higher, too. The composition of the fluid phase with respect to X_{CO_2} was derived from

Table 1. *Geological Setting of the Three Investigated Occurrences*

	Habachtal (H)		Felbertal (F)		Schrammacher (S)	
Tectonic unit	Venediger nappe[1] Untere Schieferhülle "Habachserie"[2] (lower schist cover)		Venediger nappe[1] Untere Schieferhülle "Habachserie"[2] (lower schist cover)		Venediger nappe[1] Zentral Gneis "Tuxer Kern"[2] (central gneiss core)	
Lithology	stratabound Be-W-mineralization; blackwall-zoning between serpentinites and metapelites		stratabound W-deposit; quartz-layers and biotite-plagioclase gneisses in amphibolites		Be-minerals in leucocratic orthogneiss	
Metamorphic events	pre alpine	alpine	pre alpine	alpine	pre alpine	alpine
P-T estimates	$P < 3$ kbar[4] $T < 450°C$[4]	$P = 4.5–6$ kbar[3] $T = 500–550°C$[5]	? ?	$P > 4.5$ kbar $T = 500–550°C$[5]	? ?	$P = 5–7$ kbar[6] $T \approx 550°C$[5,6]

[1] Frisch (1977), [2] Morteani (1974), [3] Grundmann (1980), Grundmann and Morteani (1982), [4] Koller and Richter (1984), [5] Hoernes and Friedrichsen (1974), [6] Selverstone et al. (1984).

fluid inclusion studies (Luckscheiter and Morteani 1980) at the Habachtal for beryl and phenakite (Be_2SiO_4). They vary between 0.03 and 0.07. We do not want to imply, that the P-T conditions summarized in Table 1 are those under which the beryls were formed, but they are very likely the conditions which led to the main mineral assemblages of the rock. The specific beryl forming process will be discussed later.

Results

1. Petrography

The mineral assemblages of the samples investigated and some details about the textural relationship of the beryls are summarized in Table 2.

Felbertal: The beryl-bearing rock series are quartzitic rocks to mica schists, intercalated within a thick unit of paleozoic amphibolites and biotite-plagioclase gneisses (the Habach series). The samples come from the Mittersill scheelite mine, which is a metamorphosed, probably sedimentary stratiform tungsten deposit according to Höll (1975) who described the local geology in detail. All of the Felbertal samples are very quartz-rich. Mica (mostly phengite) and calcite are abundant. Fluorite, sulfides and phenakite are characteristic minerals, which are present in varying amounts. Beryl occurs as a normal constituent of gneisses and schists, but is more abundant in veins and knauer-type rocks. The term "vein" describes a small (cm-size) layer of predominantly quartz, sometimes folded (sample no. F16), in schistose to gneissic rocks, whereas "knauer" means a segregation of (mostly) quartz of irregular shape, often lense-shaped (of the order of 10–20 cm). Both types of rock do not show any cavities or druses, and we think that they do not represent late stage hydrothermal mineral assemblages of the alpine metamorphism. All mineral phases seem to be in textural equilibrium except phenakite, which is always rimmed by beryl (see Figs. 2 and 3). The beryls are mostly anhedral, macroscopically blue (except sample no. F53, which is bright yellow), colorless in thin section (except F53: yellow).

Habachtal: The beryl-bearing rocks are situated in a narrow zone between serpentinites and metapelites/metavolcanics. This zone was strongly influenced by metasomatism ("black wall zoning"), and the beryls occur mostly in biotite-, talc-, and actinolite-schists. Though it lies near to the central gneiss core, which consists of orthogneisses, no genetic relationship between these and the beryl-bearing rocks exist. The local geological situation is described in detail by Grundmann (1983) and Grundmann and Morteani (1982). The beryls occur generally in quartz-poor rocks (except samples no. H60 and no. H154, which are knauers of the same type as mentioned above). Biotite, chlorite, actinolite, talc, plagioclase, and epidote are the most abundant minerals. Among the minerals of the epidote group, allanite occurs frequently. All major phases seem to be in textural equilibrium, again with the exception that phenakite is rimmed by beryl, but only two samples have relict phenakite (see Fig. 3). Most of the beryl crystals are euhedral, colorless to greenish, sometimes emerald-green, in

Table 2

Sample No	Rock type	qtz	pla	kfs	bio	mus	chl	act	epi	gt	cc	ph	ap
H 3	mus-schist		o		o	∮	-		o				
H 29	act-schist				∅			∮					-
H 40	bio-schist				∮		∅		o				-
H 54	bio-chl-schist				∅	∅	∮		o				
H 60	act-qtz-knauer	•			-			∅					-
H 85	pla-chl-mus-schist		∅		/	∅	∅		o				-
H 100	bio-epi-plag-gneiss	o	o		∅		/		o				-
H 102	chl-bio-mus-schist		o	/	∅	∅	∅		o		/		-
H 104	bio-schist				∮	-			o				o
H 128	talc-schist				∅			∅					
H 150	bio-schist		o		∮		-						
H 151	bio-schist				∮								
H 152	bio-act-schist				∮			∮					
H 153	bio-chl-schist				∅		∅		-			∮	
H 154	bio-qtz-vein	•	-		∮		o				/		
H 155	bio-schist		∅		∮	o	∅		-		/		-
H 179	bio-schist		•		∮	-	-		o		-		-
H 200	bio-chl-schist				∮		o		o			o	-
F 16	ph-qtz-vein in bio-schist	o	-		∅		-	-	o	o	∅	∅	-
F 50	bio-schist	o			∮				o		o		
F 51	qtz-pyr-vein	•			/	∅					∅	o	
F 52	qtz-mus-schist	o	o	∅		∅			∅		∅	∅	
F 53	qtz-vein	•				∅					-	∅	
F 54	ph-qtz-knauer	•									o	-	
F 55	ph-qtz-knauer	•									o	∮	
S 156	mus-gt-nodule in gneiss	o			-	∅			-	∅			
S 176	qtz-vein in gneiss	o	-		∅	∅						∅	-
S 179	gneiss	o	∅	∅	-	∅			o	o		o	
S 223	mus-gt-nodule in gneiss	o	o	∅	-	∅			o	∅		-	
S 225	gt-mus-schist	o	o	o	∅	∅				∅			-

abbreviations: act = actinolite; ap = apatite; bio = biotite; cc = carbonate (in most cases calcite, but not always verified); chl = chlorite; cph = chacopyrite; epi = epidote group; gt = garnet; kfs = K-feldspar; mol = molybdenite; mus = K-white mica; ph = phenakite; pla = albite-rich plagioclase; pyh = pyrrhotite; pyr = pyrite; qtz = quartz; sch = scheelite; tit = titanite; tur = tourmaline

vein-assemblages bluish, but colorless in thin-section. Inclusions of mica, epidote, plagioclase and many other minerals (Grundmann 1981) are very abundant, and these are oriented according to the foliation of the schistose rock. The inclusion patterns indicate zoning of the beryls, with cores rich in inclusions and rims inclusion-poor to inclusion-free. Sections parallel to the elongation of the beryls show sector zoning (Grundmann and Morteani 1982).

Schrammacher: Both of the above-mentioned occurrences lie within the

Table 2 (*continued*)

others	describtion of beryl
tur	euhedral, colorless, 5 mm,[1] sector zoned[2]
	euhedral, colorless, 5 mm, act-inclusions[3]
	euhedral, colorless, 4 mm, epi-bio-chl-inclusions, large fluid inclusions
margarite	anhedral, colorless, 4 mm
	subhedral, green, 7 mm, fluid inclusions
rutile, tur	anhedral, crystal aggregate, 1 mm, epi-pla-bio-chl-inclusions
	euhedral, colorless to yellowish, 2 mm, epi-bio-pla-inclusions, zoned
rutile, tur	euhedral, colorless, 4 mm, epi-chl-bio-kfs-inclusions, zoned
	euhedral, colorless, 1.4 mm, epi-bio-mus-inclusions, clear core
talc	euhedral, bright green, 0.3 mm
talc	euhedral, green, 4.5 mm
	euhedral, colorless to light blue, 1 mm, extremely elongated, fluid incl.
	subhedral, bright green, 3 mm, act-bio-inclusions
aeschynite	subhedral, colorless to light green, rim around large ph, fluid inclusions
	euhedral, colorless to light bluish, 2 mm, elongated fluid inclusions
	euhedral, colorless, 2 mm; at the contact pla/bio-schist
	euhedral, colorless to light green, 0.2 mm; at the contact pla/bio-schist
rutile, talc	euhedral, green, 4 mm; large ph-inclusions
tit, pyr, prh, mol	anhedral, colorless, rims around phenakite
cph, prh, sch, mol	subhedral, colorless, 1 mm; bio-epi-inclusions
fluorite, pyr	anhedral, blue, 1.5 mm; ph-inclusions
fluorite	anhedral, colorless to bluish, 2 mm; ph-mica-incl.; in cc-rich layer
tit, Pb-Bi-sulfosalts	anhedral + euhedral, yellow, 0.7 mm;
Pb-Bi-sulfosalts	subhedral, blue, 0.8 mm; fluid inclusions rich core, ph-inclusions
Pb-Bi-sulfosalts	phenakite rimmed by anhedral blue beryl
magnetite	subhedral, blue, asymmetrically zoned, 0.6 mm
	anhedral, blue; ph-inclusions; at the contact vein/gneiss
	anhedral, blue, 1.5 mm; mica- and ph-inclusions
magnetite	anhedral, blue, 0.4 mm; mica- and ph-inclusions
magnetite	subhedral, blue, 1.0 mm; mica-inclusions in core

symbols : • present in large amounts; o normal constituent; - accessories;
/ microprobe analysis

1) max. size of beryl in diameter

2) zoning is mentioned only if it is very obvious in thin section

3) inclusions are listed only if very abundant

"Habachserie" of the lower schist cover, which is of volcano-sedimentary origin, and where the influence of intrusive rocks on the formation of Be-minerals can safely be excluded. This is not the case, however, for the third locality, the Schrammacher, where beryl occurs in gneisses of the "Tuxer Kern" of the central gneiss core (Morteani 1974). This area consists of different types of orthogneisses and metamorphic overprinted migmatites. The beryl-gneiss is leucocratic with large amounts of white mica. In some areas mica-garnet-nodules

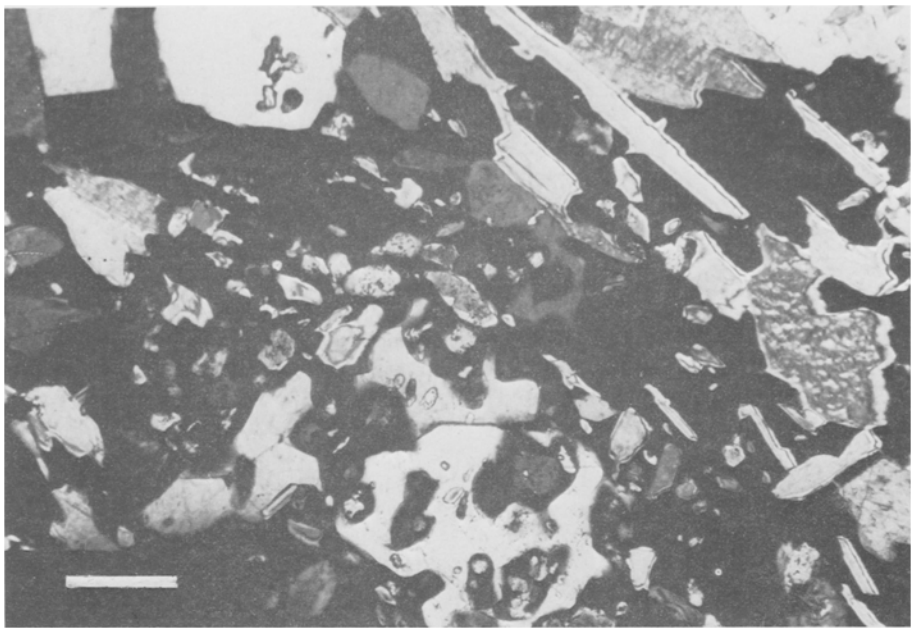

Fig. 2. Thin section photograph of poiciloblastic beryl (black) with inclusions of phenakite, phengite, quartz, and K-feldspar; sample F52; + nicols, scale bar is 0.2 mm

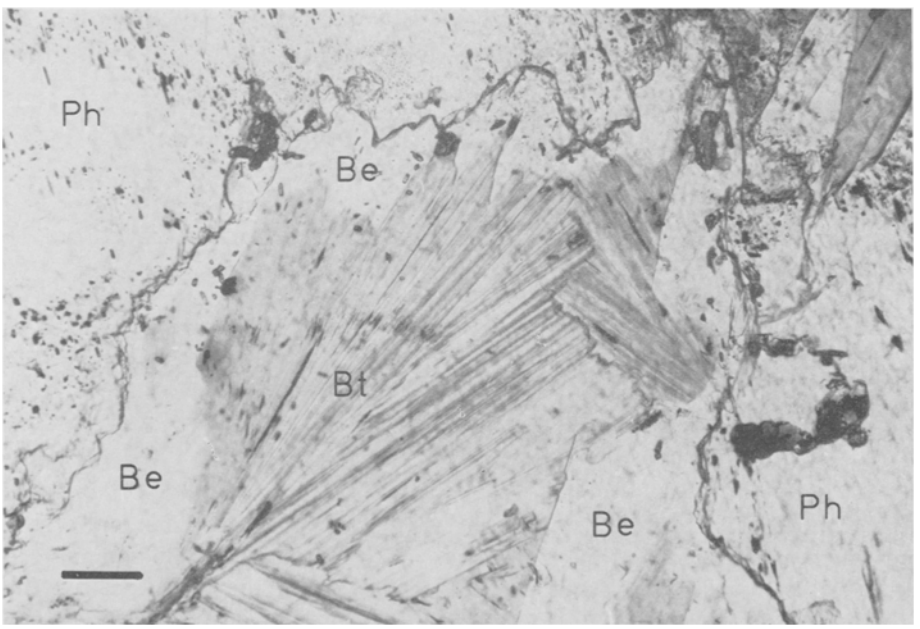

Fig. 3. Thin section photograph of two large phenakite grains (*Ph*) with interstitial beryl (*Be*) and biotite (*Bt*); sample H155, – nicols, scale bar is 0.1 mm. For pictures with typical inclusion patterns in these beryls see Grundmann and Morteani (1982)

of varying size (1–15 cm) and thin (approximately 50 cm) layers of mica-schist occur, which are often rich in beryl. Fig. 4 shows an example of such a garnet-mica nodule. It seems possible that they are pseudomorphs after a Na-Be-cordierite (Franz et al. 1984). Beryl was found, too, in the normal leucocratic gneiss and in quartz-veins. It is assumed that the oiriginal rock was a granite with pegmatitic parts representing a late, highly differentiated type. This hypothesis seems supported by the high Fe/Mg-ratio of the minerals as well as by the

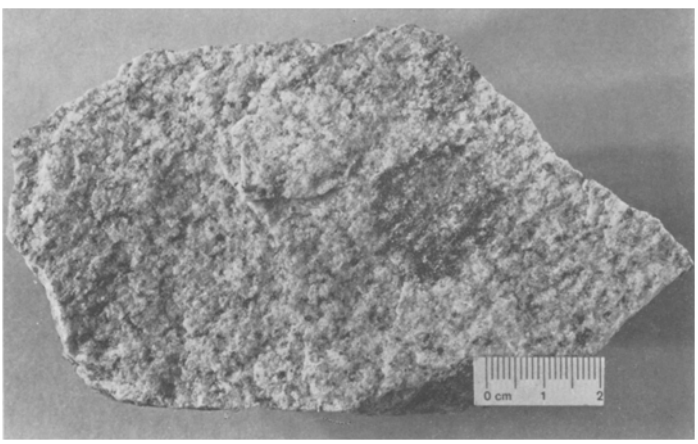

Fig. 4. Hand specimen from the Schrammacher orthogneiss with a typical garnet-phengite-beryl nodule. The light excentric core is mostly garnet, the dark margin phengite; beryls are concentrated at the border between phengite and gneiss or garnet and gneiss

high Mn-content of the garnet. The beryls occur in mineral assemblages that are characterized by a high amount of white mica (a phengitic green muscovite). Garnet and magnetite are typical minerals here which were not observed in most of the samples from the other two localities. Again phenakite was observed only as a relict phase included in beryl, and all other phases seems to be in textural equilibrium. The beryl crystals are mostly subhedral and poikiloblastic; macroscopically and in thin section they are pleochroic blue to colorless. Mica inclusions are abundant, sometimes concentrated in the core of the crystals. Zoning in color was observed, too, where the intensity of the color increases towards the rim. One sample (S156) shows asymmetrical zoning with a blue rim towards muscovite and a colorless rim towards quartz.

2. Mineral Chemistry

2.1 Analytical Technique

Analyses were performed with an electron microprobe (Siemens Elmisonde) connected with two fully focussed spectrometers (WDS) and with KEVEX energy dispersive system (EDS). Operating conditions were 18 kV accelerating

voltage, 100 nA (WDS) and 2.5 nA (EDS) probe current, and a 1 μm beam diameter. During the intensity measurements (WDS) thin sections were moved 2 μm; counting time was 3×12 seconds. Synthetic MgO, Al_2O_3, TiO_2, Cr_2O_3, metallic Mn, Fe, wollastonite (Si, Ca), jadeite (Na), and K-glass served as standards, ZAF correction programs were used.

In order to detect compositional zoning from grain core to rim, several point analyses were carried out on traverses across mineral grains. Analyses for the outermost margin are taken ~ 10 μm from the grain border. The microprobe technique is the only standard method which allows determination of element compositions of small areas like inclusions (see Fig. 3) and border zones (e.g. phenakite rimmed by beryl, see Fig. 2). This method has the disadvantage of being unable to detect light elements. Therefore the major element Be in beryl cannot be determined by this technique and also the important minor element Li as well as H_2O.

2.2 Beryl

Representative microprobe analyses and calculated formulas are compiled in Table 3. All data – approximately 120 point analyses in 32 different samples – are included in the figures. There are several problems in calculating the beryl formula from partial microprobe analyses:

- BeO, Li_2O, and H_2O are not determined.
- The oxidation state and position of Fe in the beryl structure is unknown.
- The number of cations per formula unit varies due to the vacany in the beryl channels; furthermore, it is unknown whether in addition to alkalies Fe, Mg, Ca may be accomodated in these channels, too.
- All the major elements Be, Al, and Si can theoretically be placed into tetrahedral sites; this allows several substitution mechanisms (including combined substitutions with other elements in octahedral positions or within the channel site) and it is therefore impossible to design any element with a known stoichiometric coefficient.

We therefore choose the following procedure. Beryl formulas were calculated in two different ways. Firstly, we normalized to Si = 6.00, neglecting the beryllium content (see Table 3). Secondly, we calculated the formula on the basis of 18 oxygens, assuming an ideal stoichiometric BeO-content of 13.3 wt.% (for beryl with approximately 2 wt.% Na_2O, 3 wt.% (MgO + FeO), and 2 wt.% H_2O). This model is based on calculations where the BeO-content had been increased by increments of 0.25% from 12–14 wt.%. It turned out that a value near 13.3 wt.% yielded the "best" formula, i.e. a formula with a coefficient for Si close to 6.0, Be close to 3.0, and the sum of octahedrally coordinated cations close to 2.0. The final comparison showed that both methods gave very similar results.

Iron was calculated as Fe^{2+} though the results suggest that some of the total Fe is likely to be present as Fe^{3+} (see discussion). Recalculation with Fe_{tot} as Fe^{3+} does not change significantly the Si:Be:Al ratio (since Fe_{tot} is low), but is of course important for coupled substitutions involving octahedral sites. This will be discussed below. Though H_2O is present in these types of beryl with

Table 3. *Representative Microprobe Analyses of Beryl and Structural Formulas, Normalized to Si = 6.00*

Sample[1]	H 128c	H 128m	H 60 m	H 100c	H 100m	H 3	H 152c	H 152m	H 40c	H 40m	H 200c	H 200m
SiO_2	62.8	62.3	62.7	63.2	62.8	63.0	63.7	63.8	63.4	63.3	64.4	64.3
Al_2O_3	13.00	12.5	13.4	14.4	13.9	14.2	14.5	14.3	15.1	14.5	15.5	14.7
Cr_2O_3	0.03	0.03	0.06	–	0.02	0.02	0.31	0.36	–	0.03	–	–
MgO	3.10	3.21	2.74	2.38	2.80	2.53	2.26	2.41	2.02	2.24	1.82	2.27
FeO^2	0.81	0.91	0.85	0.81	0.86	0.69	0.40	0.41	0.44	0.44	0.66	0.62
MnO	–	–	–	–	–	0.02	0.03	0.03	–	–	–	–
CaO	0.03	0.04	0.01	–	0.02	0.02	–	0.02	–	–	–	–
Na_2O	2.15	2.26	1.69	1.89	1.94	2.42	2.03	2.00	1.69	1.88	2.26	2.66
K_2O	0.01	0.01	0.01	0.01	0.03	0.03	0.01	0.01	0.01	0.01	–	–
Σ	81.93	81.26	81.46	82.69	82.37	82.93	83.24	82.93	82.66	82.10	84.64	84.55
Al	1.46	1.43	1.52	1.61	1.56	1.59	1.61	1.58	1.69	1.62	1.70	1.61
Mg	0.44	0.46	0.39	0.38	0.40	0.36	0.32	0.34	0.28	0.32	0.25	0.32
Fe^{2+}	0.06	0.07	0.07	0.06	0.07	0.05	0.03	0.03	0.04	0.04	0.05	0.05
Σ^{VI}	1.96	1.96	1.98	2.02	2.05	2.00	1.99	1.98	2.00	1.97	2.00	1.98
Na	0.40	0.42	0.31	0.35	0.36	0.45	0.37	0.37	0.31	0.35	0.41	0.48

Table 3 (*continued*)

Sample[1]	F 16m	F 50	F 51	F 53m	F 55c	F 55m	S 225c	S 223	S 156c	S 156m	S 179c	S 179m
SiO_2	61.3	63.1	63.6	64.4	65.7	65.4	61.7	64.7	66.2	65.0	64.8	63.4
Al_2O_3	12.8	13.2	13.8	14.9	17.2	15.7	15.0	15.7	17.4	16.6	18.2	14.0
Cr_2O_3	0.02	–	–	–	–	–	0.02	–	–	–	–	–
MgO	2.80	2.34	2.03	1.42	0.65	1.78	0.71	0.48	–	–	1.10	1.67
FeO[2]	1.48	1.60	1.65	1.30	1.05	0.92	2.52	3.64	2.45	2.58	0.82	3.70
MnO	0.03	–	–	–	–	–	0.02	–	–	0.08	–	–
CaO	0.03	–	–	–	–	–	0.01	–	–	–	–	–
Na_2O	2.44	2.43	2.47	1.89	0.25	1.73	0.85	1.52	–	1.58	0.40	2.24
K_2O	0.06	0.04	–	–	–	–	0.06	–	0.14	–	–	–
Σ	80.96	82.71	83.55	83.91	84.85	85.53	80.89	86.04	86.19	85.84	85.32	85.01
Al	1.48	1.48	1.52	1.64	1.85	1.70	1.72	1.72	1.86	1.81	1.98	1.57
Mg	0.41	0.33	0.29	0.20	0.09	0.24	0.10	0.07	–	–	0.15	0.23
Fe^{2+}	0.12	0.13	0.13	0.10	0.08	0.07	0.20	0.28	0.19	0.20	0.06	0.29
Σ^{VI}	2.01	1.96	1.94	1.94	2.02	2.01	2.02	2.07	2.05	2.01	2.18	2.09
Na	0.46	0.45	0.45	0.34	0.05	0.31	0.16	0.27	–	0.28	0.07	0.41

[1] c = core, m = margin. [2] $Fe^{2+} = Fe_{tot}$.

TiO_2 is in most cases below detection limit; formula coefficients for Cr, Mn, Ca, and K are mostly below 0.005.

2–2.5 wt.% (Franz 1982), the formulas were calculated on an anhydrous basis, because this water is present as H_2O and not as $(OH)^-$ in beryl (Wood and Nassau 1968). The same should apply for CO_2 if present in these channels.

The small Li_2O-contents are neglected. Previous determinations by AAS (Franz 1982) for some Habachtal beryls yielded 0.02–0.06 wt.% Li_2O. We

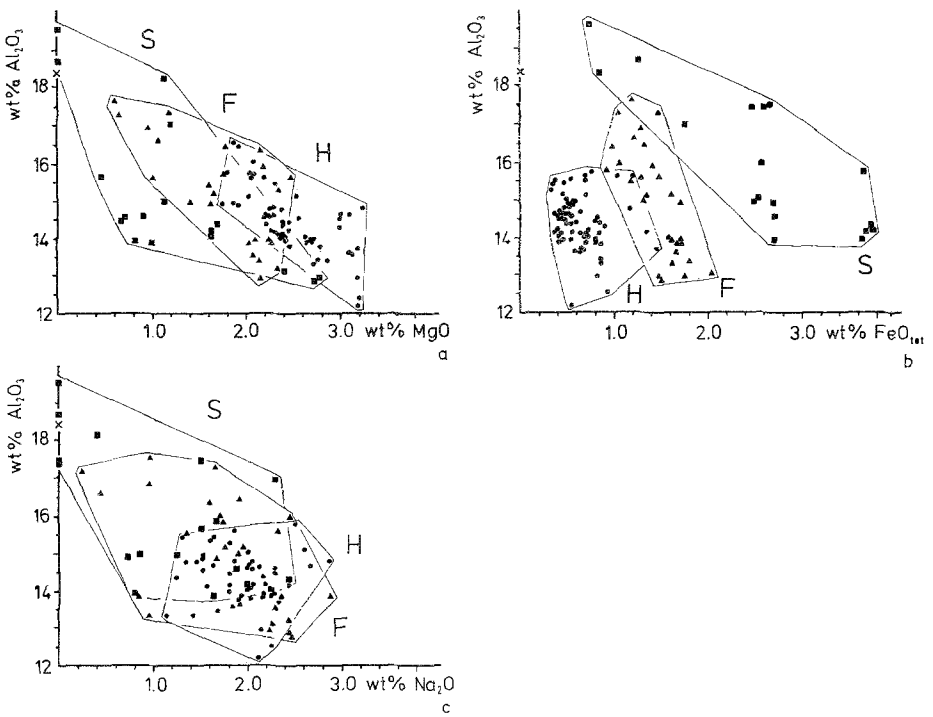

Fig. 5 a, b, c. Correlation of Al_2O_3-contents with MgO (a), FeO (b), and Na_2O (c) (wt.%) for analyses of all beryl samples (dots = Habachtal, *H*; squares = Schrammacher, *S*; triangles = Felbertal, *F*; the same symbols are used in all following diagrams)

assume that most of the beryls from this area have Li_2O-contents in the same order of magnitude, since whole rock analyses showed very low and constant Li_2O values. The same may be assumed for the Felbertal beryls, since they occur in a rather similar rock sequence of the same lithostratigraphic position (see Table 1). It is possible that the Schrammacher beryls have higher Li_2O-contents, since they are probably of primary pegmatitic origin, where high Li-contents are observed frequently (Beus 1966).

The SiO_2-content is rather constant for the Habachtal beryls. It varies between 62 and 63 wt.%, only a few analyses show values up to 66 wt.%. The SiO_2-content for the Felbertal beryls is less constant and varies between 61.5 and 65 wt.%, and for the Schrammacher beryls between 61 and 67.5 wt.%. No systematic change in composition from core to rim was observed.

The Al_2O_3-content is very variable in all samples and ranges from 12.5–18.5 wt.%. Only some of the samples (cores) from Schrammacher have Al_2O_3-contents near to the ideal value, all other samples are significantly depleted in Al_2O_3. Deficiency of aluminium is always correlated with high contents of MgO (Fig. 5a). Similarly a negative correlation between Al_2O_3 and FeO exists for the Schrammacher beryls and for the Felbertal beryls (Fig. 5b), but not for the Habachtal beryls. Na_2O is also negatively correlated with Al_2O_3, though with a large scatter independently from the locality (Fig. 5c). Chemical zoning

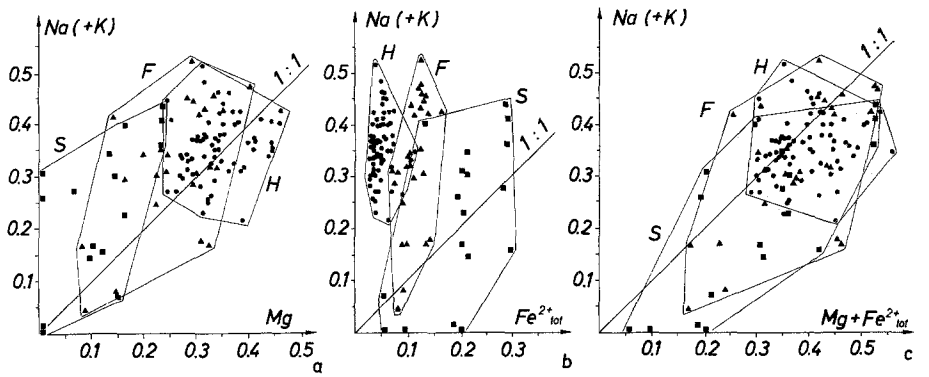

Fig. 6 a, b, c. Correlation of alkalies (mostly Na, only minor amounts of K are present) of beryl with a) Mg, b) Fe^{2+}_{tot}, and c) $(Mg+Fe^{2+}_{tot})$ in stoichiometric coefficients. a) Shows that in many cases Mg < Na, requiring another cation for charge balance. b) Shows that Na varies indipendently from Fe^{2+}_{tot} (only the Fe-rich samples from Schrammacher show a slight positive correlation), but that each locality has its typical range of Fe-contents. c) Shows that $Mg+Fe^{2+}_{tot}$ is mostly higher than Na(+K), which implies that part of the Fe_{tot} must be present as Fe^{3+}

is such that the cores are always richer in Al_2O_3 than the rims. The only exceptions are where annealed cracks cut the beryl. In such cases the composition of the beryl adjacent to the crack is similar to the rim composition.

MgO, FeO, and Na_2O, which are not necessary constituents of beryl, are present in almost all of the samples. The only exceptions are among the Schrammacher beryls with high SiO_2- and Al_2O_3-contents. In contrast to the correlations shown in Fig. 5 only the samples from H and F suggest a weak correlation between MgO and FeO. The three occurrences can, however clearly be distinguished by their different Fe/Mg ratios (see also discussion below). Mg is positively correlated with Na (+ K) for all three occurrences (Fig. 6a) although considerable scatter is apparent. If Mg < Na, this requires another cation for charge balance. Fig. 6b suggests an increasing correlation between Na (+ K) and Fe^{2+}_{tot} with the absolute amount of Fe_{tot} typically increasing from the H to the F and the S beryls. Fe^{2+}_{tot} may be positively correlated with Na for the S beryls and – possible also – for the F beryls, but no correlation is found for the H beryls. Mg + Fe^{2+}_{tot} is mostly higher than Na (+ K), which implies that part of the Fe^{2+}_{tot} must be present as Fe^{3+} (Fig. 6c).

Minor elements in the beryls include Cr_2O_3, which was observed in small amounts (0.02 wt.%, rarely up to 0.3 wt.%) in the Habachtal samples, mostly enriched in the rim. *MnO* is always very low, on the order of 0.02 wt.%, even if the beryls coexist with spessartine rich garnet. K_2O is very low, too, in the order of 0.01 wt.%, as well as *CaO*. TiO_2 is mostly below detection limit (< 0.01 wt.%).

Since the major element BeO cannot be determined by microprobe analyses, and since most beryls contain up to 3 wt.% H_2O ($\approx$ 1 H_2O per formula unit)

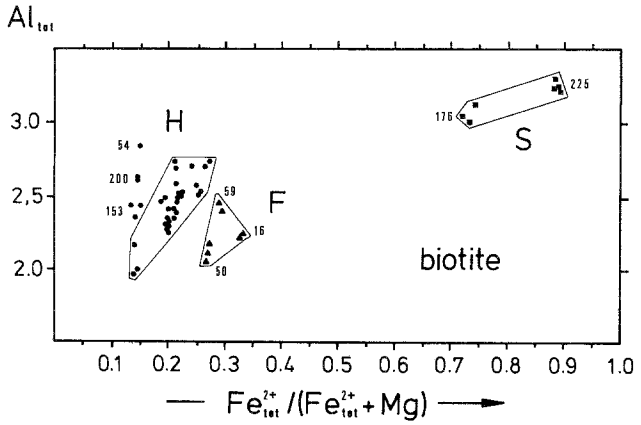

Fig. 7. Stoichiometric coefficient of Al_{tot} (= Al^{IV} + Al^{VI}) in biotite coexisting with beryl, plotted against $Fe^{2+}_{tot}/Fe^{2+}_{tot}$+Mg. Each locality has its typical Fe/Mg ratio (see text, and compare with Fig. 10 for beryl)

(Beus 1966; Franz 1982), it is difficult to check the accuracy of the analyses by evaluating the *total*. It varies between 81 and 86 wt.%. This is a fair value, if one accounts for some 2–3 wt.% H_2O, ~ 13.3 wt.% BeO, and possible other minor elements in the range of 0.X wt.%.

2.3 Coexisting Minerals

It is one of our aims to correlate the composition of beryls with the mineral assemblages of the host rock. Therefore the composition of the coexisting minerals is described in the following section. Sample numbers (see Table 2) are given in brackets.

Plagioclase from Habachtal is either pure albite with *An*2 (H155) or *An*20 (H3); from Schrammacher it is albite with *An*2 (S179).

K-feldspar (H102, S179, S223) has albite components (Na/Na + Ca + K) of up to 10 mol.%, in Felbertal Na_2O is below detection limit (F52).

Biotite is very often the major constituent in the Habachtal samples and an important mineral in many others. They are characterized by a large variation

in Fe/(Fe+Mg) ratios and a large variation in Al-content (see Fig. 7). As in the case of beryl, the three localities can be distinguished by their different Fe/(Fe+Mg) ratios in biotite: Low to intermediate ratios are typical for Habachtal, intermediate ratios typical for Felbertal, and high ratios typical for Schrammacher. The variation for all biotites ranges from almost pure phlogopite to Al-annite. With increasing Fe/(Fe+Mg) ratios, the Al-content increases within each group. Exceptions from this general trend are some of the Habachtal samples (H54, H153, H200), which have either relic phenakite or margarite in the assemblage, and thus differ from all of the other Habachtal samples. These biotites are inclusions in beryl, and compared to the other biotites, rich in Al, though they have a rather low Fe/(Fe+Mg) ratio. The biotites show typical ranges of composition for each rock type. With increasing Fe-contents these are: Talc schist, actinolite schist, biotite schist, chlorite schist, muscovite-plagioclase gneisses and schists.

Muscovite occurs at all three localities. It is phengitic with a "phengite content" P = (Mg+Fe)/sum oct)×100 ranging from 11 to 22 (Habachtal), 20 to 33 (Schrammacher) and 18 to 35 (Felbertal), or in terms of Si-content per formula unit, 6.3 to 6.8 (Habachtal), 6.3 to 6.7 (Schrammacher), and 6.5 to 7.1 (Felbertal). Fe/(Fe+Mg) ratios are as variable as those of the biotites, but between these two minerals, Mg is preferably incorporated into phengite. Na- and Ca-contents are mostly low.

Margarite was observed in one sample only (H54). According to X-ray data (Grundmann 1980) and low totals for microprobe analyses, it is a Be-rich variety.

Talc is limited to the Habachtal locality, and there it is found in two samples only. They have 0.40 and 0.46 Fe per formula unit (calculated on the basis of 22 oxygens) and very small amounts of Na (0.03) and Al (0.06).

Chlorite is present in the Habachtal samples, mostly. Coefficients for Si (calculated on the basis of 28 oxygens) vary from 5.3 to 5.6, and the Fe/(Fe+Mg) ratio varies from 0.15 to 0.26. According to the nomenclature given by Hey (1954) they are sheridanite-ripidolite. Fe/(Fe+Mg) ratios are almost the same for coexisting biotite and chlorite.

Amphiboles from Habachtal are actinolites (Leake 1978) with Si-coefficients 7.63 to 7.95, Ca ranging from 1.65 to 1.92, up to 0.15 Na filling the B-site, and Na plus K in the A-site summing up to 0.08 to 0.25. The Fe/(Fe+Mg) ratio is rather constant, between 0.135 and 0.18.

Epidote is a typical accessory phase especially for the Habachtal samples and has 50% pistazite endmember.

Garnet was analyzed in the Schrammacher samples. It is very variable in composition in different samples and from grain to grain within one sample. Two small garnet grains lying on the opposite side of a beryl (sample S156) have *Gro*35/*Spe*11/*Alm*54 and *Gro*18/*Spe*32/*Alm*50, respectively, within one grain (S223) *Gro* varies from 30 to 35, *Alm*41 to 35, and *Spe* is constant with 29. Sample S225 has *Gro*19, *Spes*10, *Alm*70. Mg-contents are always very low with a pyrope content below 1%.

Phenakite is always very pure, and besides SiO_2 with a value close to the ideal, no other elements were detected by microprobe analyses.

Discussion

1. Crystal Chemistry of Beryl

1.1 The Structure of Beryl

$Al_2Be_3Si_6O_{18} \cdot n(H_2O, \ldots)$, contains nine tetrahedrally coordinated cations per formula unit, normally occupied by Be and Si, and two octahedrally coordinated cations, normally occupied by Al. In addition, there are two non-stoichiometric positions in the channels available which are formed by the Si_6O_{18}-rings stacked parallel to the crystallographic *c*-axis. One is at the center of the six-membered rings at (000), the other lies between two Si_6O_{18}-rings at $(00\frac{1}{4})$ (Gibbs et al. 1968), with an approximate diameter of 2.8 and 5.1 Å (Wood and Nassau 1968), respectively.

1.2 Major Substitutions

The analyses of beryls from the three localities and calculated formulas show that in most cases Al coefficients are much smaller than 2.00. Furthermore, Mg, Fe, and Na are present in large amounts. Mg and Fe are negatively correlated with Al, and this suggests replacement of Al by Mg and Fe. This substitution requires a charge balance, and since Mg and Na are positively correlated (Fig. 6a), we may assume the substitution:

$$Al^{3+,VI} + \square^{channel} = Mg^{2+,VI} + Na^{+,channel}.$$

If this type of substution is strictly valid, the plot Mg versus Na in Fig. 6a should yield a line with 1:1 slope (small amounts of K present in several samples, are combined with Na, assuming that both alkali elements behave similarly). It is obvious from this figure that most of the data lie above the 1:1 line, especially the Fe-rich samples from Schrammacher and Felbertal. This indicates an excess of Na which requires another coupled substitution. Most likely this is:

$$Al^{3+,VI} + \square^{channel} = Fe^{2+,VI} + Na^{+,channel}$$

(provided no other monovalent cation is involved).

Nevertheless, in a plot Na versus Fe (all Fe calculated as Fe^{2+}), only the Fe-rich samples from Schrammacher show a slight positive correlation near to the 1:1 line (Fig. 6b). For the other two localities Na seems to vary independently from Fe.

If the sum of Mg and Fe_{tot} is plotted versus (Na+K) (Fig. 6c) many analyses lie below the 1:1 line. This indicates that not all Fe is necessarily present as Fe^{2+} to compensate Na (if no other nondetected monovalent cations are present), and that some of the Fe is present as Fe^{3+}, incorporated into beryl by the simple substitution

$$Al^{3+,VI} = Fe^{3+,VI}.$$

In Fig. 8 all data are plotted in a diagram (Al+Cr) versus ($Mg+Fe^{2+}_{tot}+Na+K$). Most of the data lie near to the line which corresponds to the substitution

$$R^{3+,VI} + \square^{channel} = R^{2+,VI} + R^{+,channel}.$$

If Fe is calculated as Fe^{3+} and plotted together with Al, the general picture is

the same, because the data points move only more or less parallel to the line towards higher R^{3+} and lower $(R^{2+} + R^{+})$ values. A few samples deviate from this trend: H128 and H60 fall clearly below the line. Interestingly, both represent extremely Al-poor bulk rock compositions (talc-schist and actinolite-quartz-

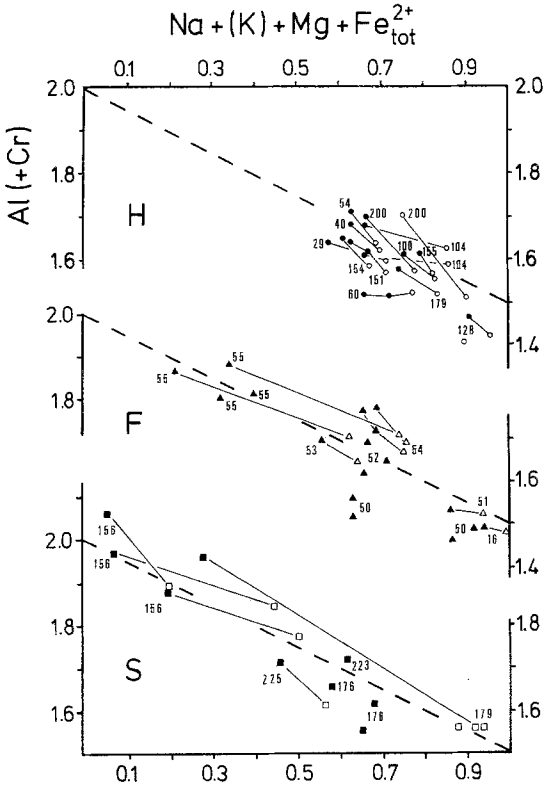

Fig. 8. Stoichiometric coefficients of Al (+ Cr) plotted against ($Na+K+Mg+Fe^{2+}_{tot}$) for the Habachtal, Felbertal, and Schrammacher beryls. Filled symbols indicate core, open symbols indicate margin composition, isolated filled symbols indicate analyses from crystals with no clear core/margin relationships. The dashed line corresponds to the ideal substitution $R^{3+} + \square = R^{+} + R^{2+}$. Numbers indicate sample numbers

knauer). Several analyses (S156, S179, S223, F54) lie above the line. In all these cases (and probably for all the minor deviations, too, if they are not caused by analytical uncertainties other substitutions may be responsible, such as:

$$Be^{2+,IV} + Si^{4+,IV} = 2\,Al^{3+,IV}$$
$$Si^{4+,IV} + \square^{channel} = Al^{3+,IV} + R^{+,channel}$$
$$Si^{4+,IV} + \square^{channel} = Be^{2+,IV} + 2\,R^{+,channel}$$

or by minor substitutions involving Li.

The variation of the elements Al, Fe, Mg, and Na is also presented in triangular diagrams (Fig. 9a–d), showing a) the rather constant Mg/Na ratio

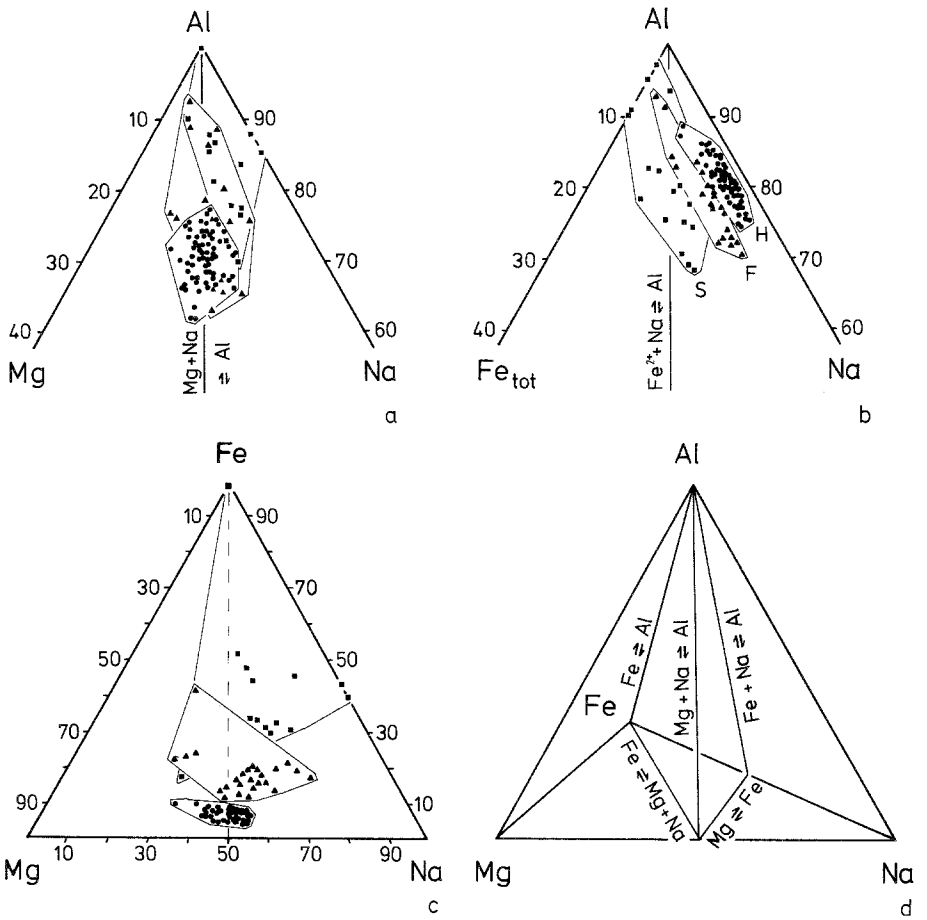

Fig. 9 a, b, c, d. Variation in chemistry of beryls of Al, Mg, Fe_{tot}, and Na (a, b, c) presented in projections on three faces of the tetrahedron Al-Mg-Fe-Na (d). Note different scale of triangles. The triangle Al-Mg-Na (Fig. 9a) shows a general trend according to the substitution Al + □ = Mg + Na (see tetrahedron). In the projection onto the Fe_{tot}-Na-Al triangle (Fig. 9b) most of the analyses fall towards the Al-Na side, indicating that the substitution Al + □ = Fe^{2+} + Na is operative to a minor extend than the coupled Mg-Na substitution. Analyses which plot near the Fe-Al side indicate the substitution Fe^{3+}-Al. Data points outside the triangle Fe-$Fe_{50}Na_{50}$-$Mg_{50}Na_{50}$ (Fig. 9c) indicate other substitutions (see text)

(except for Mg-poor, Fe-rich samples) for varying Al-contents, b) the constant Fe-contents of beryls for each locality, most pronounced for the H-samples, less evident for the F-samples and the S-samples (i.e., in this case Fe is partly correlated with Na, if it substitutes for Al) c) scatter of all data points in the diagram Mg-Fe-Na. If the only substitutions were

$$Al^{VI} + \square^{channel} = Mg^{VI} + Na^{channel}$$
$$Al^{VI} + \square^{channel} = Fe^{2+,VI} + Na^{channel}$$
$$Al^{VI} = Fe^{3+,VI}$$

all points should lie in the subtriangle of Fig. 9c Fe; Mg50/Na50; Fe50/Na50 (projected from Al, Fig. 9d). Higher Na-contents can be explained by substitution where Na is incorporated for charge balance for replacement among tetrahedral sites (see above) or by interaction with the relatively mobile fluid components, which are also present in the channels. Higher Mg and Fe contents are more difficult to explain and require Mg or Fe in beryl channels (Goldman et al. 1978; Blak et al. 1982).

1.3 Zoning in Beryl

Most samples show chemical and optical zoning (indicated by inclusions and by color). The chemically most strongly zoned crystals are from Schrammacher. In all cases where euhedral single crystals without cracks or subgrain boundaries were cut near the center, Al decreases towards the margin and the sum of ($Mg+Fe^{2+}_{tot}+Na$) increases (Fig. 8). The composition of beryl near to an annealed crack is similar to the general margin composition. The zoning is continuous for H and S with a small ($\sim 50\ \mu m$) discontinuous outermost rim, where Al again increases. The F-beryls are characterized by discontinuous zoning: Al-rich, Fe-poor cores; sharp discontinuity; Al-poor, Fe-rich wide margin with a continuous outer rim, where both Al and Fe decrease slightly.

These data suggest that the substitution reaction

$$R^{3+} + \square = R^{+} + R^{2+}$$

was operative during the whole mineral forming process. Furthermore no pervasive diffusion process took place, except in mineral volumes which had been made mechanically accessible by cracking. For the H- and F-beryls Mg is the governing R^{2+}-ion. While the Fe-content changes little, Mg increases towards the rim most markedly. This may possibly relate to the changing conditions during the metamorphic process (see below). In the S-beryls Fe is the major substituent for Al, and consequently the substitution was

$$Al + \square = Na^{+} + Fe^{2+}$$

increasing during the crystal growth. A closer inspection of the data shows, however, that the substitution is more complex: A sample with a very constant and throughout high Fe-content (S156; 2.45 wt.% FeO_{tot}, core, to 2.59 wt.%, margin) has Na_2O-contents below the detection limit in the core, but medium to high contents in the rim. This suggests that in the core the predominant substitution is

$$Al^{3+} = Fe^{3+}$$

but with increasing Na-content towards the rim was correlated with reduction of Fe^{3+} to Fe^{2+}.

So far the substitutions have been treated as exchange reactions without regarding the coexistence with other phases of the rock. Chemical zoning of the beryls may be considered as a historical record of changing chemical potentials during the rock formation because of changing P-T conditions, but possibly also due to an influx of a fluid phase. The zoning can therefore also be formulated as an exchange reaction with other minerals present during the growth of beryl,

for example with phengite, muscovite and albite

$$\underset{be}{Al_2Be_3Si_6O_{18}} + \underset{ab}{NaAlSi_3O_8} + \underset{phe}{KMgAlSi_4O_{10}(OH)_2} = \underset{be}{NaMgAlBe_3Si_6O_{18}} + \underset{qtz}{4\,SiO_2} + \underset{mus}{KAl_3Si_3O_{10}(OH)_2}$$

or with biotite/eastonite and albite

$$\underset{be}{Al_2Be_3Si_6O_{18}} + \underset{ab}{NaAlSi_3O_8} + \underset{bio}{KMg_3AlSi_3O_{10}(OH)_2} = \underset{be}{NaMgAlBe_3Si_6O_{18}} + \underset{qtz}{4\,SiO_2} + \underset{eas}{KMg_2Al_3Si_2O_{10}(OH)_2}$$

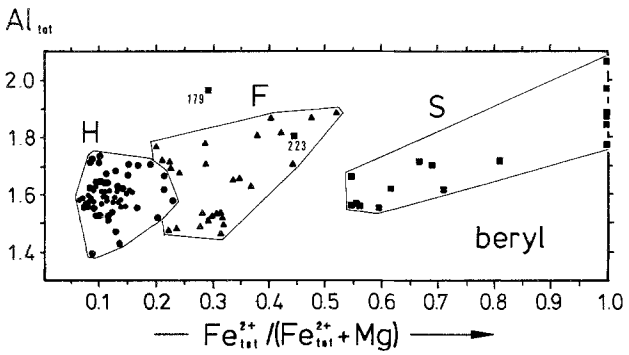

Fig. 10. Variation of Al-content of beryl with Fe/(Fe+Mg) ratio. Each locality has its typical range of Fe/Mg values (compare with Fig. 7)

or with chlorite and albite

$$\underset{be}{Al_2Be_3Si_6O_{18}} + \underset{ab}{NaAlSi_3O_8} + \underset{chl}{Mg_8Al_8Si_4O_{20}(OH)_{16}} = \underset{be}{NaMgAlBe_3Si_6O_{18}} + \underset{qtz}{SiO_2} + \underset{chl}{Mg_7Al_{10}Si_3O_{20}(OH)_{16}}$$

Thus, the exchange $Al_1\,Mg_{-1}\,Na_{-1}$ in beryl is accompanied by an exchange of $Mg_1\,Si_1\,Al_{-2}$ in sheet silicates and a consumption of albite.

2. Beryl Composition and Coexisting Minerals

It was shown for biotite that there exists a clear relationship between biotite composition (Al-content and Fe/Mg ratio) and rock type, i.e. bulk rock composition (see Fig. 7). A very similar relationship exists between beryl composition and bulk rock composition (see Fig. 10). Each occurrence has its typical range of Fe/Mg and it is obvious that especially the Fe/(Fe+Mg) ratio of the beryl is related to the rock type (see also Figs. 3, 5, 8, 9b).

The partitioning of Fe_{tot} and Mg between beryl and coexisting mica, garnet, and chlorite is shown in Fig. 11. X_{Mg} = Mg/(Mg+Fe) decreases in the order beryl > phengite > biotite > garnet for the Schrammacher. For the Habachtal X_{Mg} decreases in the order beryl ≃ talc ≥ actinolite > biotite ≃ chlorite > phengite. For the Felbertal area the samples show a decrease in X_{Mg} from phengite ≥ beryl ≥ biotite.

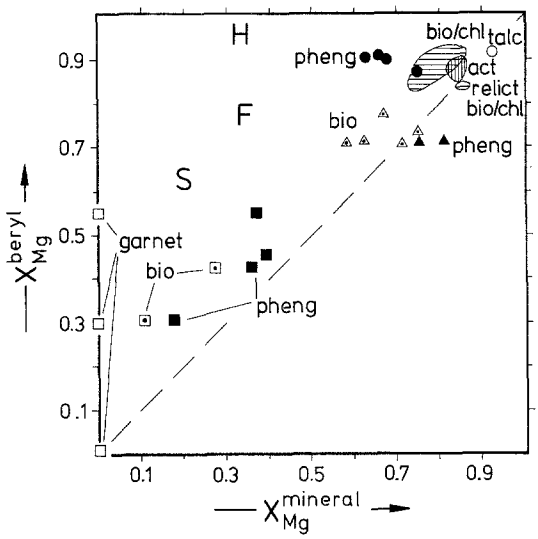

Fig. 11. X_{Mg} = Mg/(Mg+Fe^{2+}_{tot}) in beryl plotted against X_{Mg} of coexisting Fe-Mg minerals (garnet, biotite, chlorite, phengite, tremolite, talc)

All these partitioning data cannot be related to a simple exchange reaction Mg = Fe^{2+}, since all the minerals may have some of the Fe_{tot} present as Fe^{3+}. The only conclusion which can be drawn from these data is, that between all analyzed Fe, Mg-minerals, beryl has the highest Mg/Mg+Fe_{tot} ratio (except for talc and some phengites) indicating, that the substitution $Na_1 Mg_1 Al_{-1}$ is prefered compared to $Na_1 Fe^{2+}_1 Al_{-1}$ and $Fe^{3+}_1 Al_{-1}$ in beryl.

3. The Petrogenesis of Beryl

The formation of beryl in metamorphic rocks is restricted to areas with anomalously high BeO-contents: 1) In the *Felbertal*, beryllium enrichment is supposedly due to a primary sedimentary-volcanogenic process (together with tungsten) which was later concentrated in vein- and knauer-assemblages as phenakite (and possibly beryl, too). 2) In the *Habachtal* beryllium was enriched in biotite, white mica and feldspar (or, less abundant, as phenakite) within a metasedimentary/metavolcanic rock series, which was mobilized during a later metasomatism between these rocks and adjacent serpentinites, and was precipitated in the form of beryl (Grundmann 1983). 3) In the *Schrammacher* area beryllium was en-

riched in pegmatitic to granitic rocks, probably as beryl or (in veins) as phenakite, or as a minor element in cordierite.

Textural criteria, crystal chemistry of beryl and of other minerals, together with general information of the geology of the area, allows us to give some constraints about the mineral forming process. The main observations on which our reasoning is based are summarized as follows: 1) Beryls grow over the foliation of the mostly schistose to gneissic rocks, indicating their growth after the main deformation. In some cases, however, cores of relic beryls were observed, which have a completely different orientation of inclusions than the host rock implying at least two stages of mineral growth. 2) Inclusions in beryl are the same (with a similar composition) as the minerals of the matrix (except phenakite). The concentration of included minerals decreases from the center towards the rim; generally, the outer rim is inclusion free. 3) Besides beryl, phenakite is the only important Be-bearing mineral. It is always an inclusion in beryl, or – where large crystals are present – is completely surrounded by beryl. Chrysoberyl, Be-margarite, and other rare Be-minerals were described from the Habachtal, but since they are extremely rare or fissure minerals, and no clear textural relationship between beryl and these minerals are known, they are neglected in the discussion. 4) All beryls show zoning with a significant decrease of Al towards the rim the main substitution for which is $Na_1 Mg_1 Al_{-1}$. Though the beryl composition in terms of Mg/(Mg+Fe) depends on the bulk mineral composition of the rock, the amount of substitution $Na_1 Mg_1 Al_{-1}$ is independent of the mineral assemblage.

The growth conditions for beryl are characterized by a rather low nucleation rate, which is indicated by the fact that the number of beryl crystals in a rock is low, but their size is large compared to the size of other minerals of the host rock (see Table 2, which gives the approximate diameter of the beryls; since beryls are elongated parallel to the *c*-axis the length is at least 3 to 4 times the diameter). In contrast to this, the growth rate must have been rather large at the beginning, demonstrated by the large number of inclusions in the core. The growth rate decreased significantly during the later stage, and clear rims could be formed.

The fact that phenakite is a precursor mineral prior to the formation of beryl indicates a metamorphic reaction. Relic phenakite in beryls was also observed by Abrecht and Hänni (1979) in an aplitic part of the Rotondo metagranite, Swiss Alps, similar to the Schrammacher occurrence, and in schists from three different localities (Gravelotte, Cobra, and BVB-mine) of the Leydsdorp district emerald mines (own observation), which are very similar to the Habachtal deposit. We therefore assume that the metamorphic transformation of phenakite into beryl is a general feature. For those of the *Schrammacher* beryls, which have relic phenakite preserved, the following reaction is proposed:

$$\underset{ph}{3\,Be_2SiO_4} + \underset{mus}{2\,KAl_3Si_3O_{10}(OH)_2} + \underset{qtz}{9\,SiO_2} = \underset{be}{2\,Al_2Be_3Si_6O_{18}\cdot H_2O} + \underset{kfs}{2\,KAlSi_3O_8}$$

All minerals necessary for this reaction are present in these gneisses, but in the rocks of the Habachtal, K-feldspar and quartz are generally absent. Here, the

abundance of chlorite and biotite suggests another reaction

$$3\,\underset{ph}{Be_2SiO_4} + 5\,\underset{mus}{KAl_3Si_3O_{10}(OH)_2} + \underset{chl}{Mg_{10}Al_4Si_6O_{20}(OH)_{16}}$$
$$= 2\,\underset{be}{Al_2Be_3Si_6O_{18}\cdot H_2O} + 5\,\underset{bio}{KMg_2Al_3Si_2O_{10}(OH)_2} + 2\,\underset{qtz}{SiO_2} + 6\,H_2O\,.$$

These observations indicate that phenakite (together with white mica and/or chlorite) is the typical Be-mineral for rocks formed at low temperatures and/or high pressures. The assemblage beryl + K-feldspar is characteristic for the lower to high grade amphibolite facies. It was shown experimentally and documented by field observations on metamorphosed pegmatites (Franz and Morteani 1984) that at higher temperatures near to the anatectic regime beryl + K-feldspar become unstable and that chrysoberyl is the characteristic Be-mineral in the migmatite-granulite facies.

None of the above mentioned reactions seems to be directly applicable to the rocks of the *Felbertal* where sheet silicates are not as abundant as in the other occurrences. K-feldspar is generally absent, but calcite, fluorite, and sulfides are present. Furthermore, there are often large phenakite crystals in a quartz matrix, which are surrounded by beryl; no other Al-minerals are preserved and it seems unlikely that they were ever present in the immediate vicinity. All these observations indicate a mineral forming process where a fluid phase played the dominant role and delivered the necessary amount of Al

$$3\,\underset{ph}{Be_2SiO_4} + 9\,\underset{qtz}{SiO_2} + 4\,[Al(OH)_3]_{aq} = 2\,\underset{be}{Al_2Be_3Si_6O_{18}\cdot H_2O} + 4\,H_2O\,.$$

It is not clear in which specific form Al was present in the fluid phase, but the presence of calcite and fluorite might indicate CO_2- or F-complexes.

The importance of the fluid phase for the beryl-forming process for all three occurrences is furthermore underlined by the presence of H_2O in the beryl. In addition, chemical zoning which appears very similar in most samples, no matter if a Na-mineral is present or not, may be at least partly related to that. This demonstrates that the composition of beryl is not only dependent on bulk rock composition, but also on the composition of the fluid phase, which may change significantly during the rock forming process. The formation of the late beryl rim took place under circumstances, such that the activities of Na^+ (and Mg^{2+}, Fe^{2+}) were increased in comparison to the activity of Al^{3+}. The textures of the beryls indicate that their main growths stage occurred during or after the uplift from an early high pressure to a late medium pressure ($\sim$ 5 kbar, possibly with increasing temperature). This is probably the stage of the rocks where many changes in the fluid composition occurred and where dehydration reactions took place. These fluids were able

1) to concentrate beryllium during the metasomatic process;

2) to facilitate the growth of the large crystals of beryl;

3) to supply the necessary amount of Na to the rim of the beryl in cases where no Na-mineral is present and supplying the necessary amount of Al to transform phenakite into beryl in cases where no Al-mineral is present.

Acknowledgements

We want to thank G. Morteani for his continuous help during this study and S. Thomas, who discovered the Schrammacher beryls and supplied information on the geology of the area. We are grateful to the Wolfram Bergbau- und Hütten-GmbH for the permission to visit the mine and to collect samples. The manuscript was greatly improved by critical comments by F. S. Spear (Troy, N.Y.), K. Schmetzer (Heidelberg) and P. Mirwald (Bochum). Financial aid was provided by the Deutsche Forschungsgemeinschaft (Mo 232/11-1). Part of this work is the result of the Ph. D. thesis by G. G.

References

Abrecht J, Hänni H (1979) Eine Beryll-Phenakit (Be_2SiO_4)-Paragenese aus dem Rotondo-Granit. Schweiz Min Petr Mitt 59: 1–4

Beus AA (1966) Geochemistry of beryllium and genetic types of beryllium deposits. W. H. Freeman and Company, San Francisco and London

Blak AR, Isotani S, Watanabe S (1982) Optical absorption and electron spin resonance in blue and green natural beryl. Phys Chem Min 8: 161–166

Franz G (1982) Kristallchemie von Beryll, Varietät Smaragd. Fortschr Min 60: Beiheft 1, 76–78

– Morteani G (1984) The formation of chrysoberyl in metamorphosed pegmatites. J Petrol 25: 27–52

– Grundmann G, Morteani G, Ackermand D (1984) The formation of beryllium minerals in metamorphic rocks. Abstracts 27th Int Geol Congr, Moscow 5: 44–45

Frisch W (1977) Der alpidische Internbau der Venedigerdecke im westlichen Tauernfenster (Ostalpen). N Jb Geologie und Paläontologie, Mh 1977 (11), 675–696

Gibbs GV, Breck DW, Meagher EP (1968) Structural refinement of hydrous and anhydrous synthetic beryl, $Al_2(Be_3Si_6)O_{18}$ and emerald, $Al_{1.9}Cr_{0.1}(Be_3Si_6)O_{18}$. Lithos 1: 275–285

Goldman DS, Rossman GR, Parkin KM (1978) Channel constituents in beryl. Phys Chem Min 3: 225–235

Grundmann G (1980) Polymetamorphose und Abschätzung der Bildungsbedingungen der Smaragd-führenden Gesteinsserien der Leckbachscharte, Habachtal, Österreich. Fortschr Min 58: Beiheft 1, 39–41

– (1981) Die Einschlüsse der Berylle und Phenakite des Smaragdvorkommens im Habachtal (Land Salzburg, Österreich). Der Karinthin 84: 227–237

– (1983) Die Genese der regionalmetamorphen, metasomatisch-horizontgebundenen Beryll-Mineralisationen des Habachtales, Land Salzburg, Österreich. Diss Techn Univ Berlin, Federal Republic of Germany

– Morteani G (1982) Die Geologie des Smaragdvorkommens im Habachtal (Land Salzburg, Österreich). Arch Lagerstättenforschung der Geologischen Bundesanstalt Wien 2: 71–107

Hänni HA (1980) Mineralogische und mineralchemische Untersuchungen an Beryll aus alpinen Zerrklüften. Diss Univ Basel, Switzerland

Hey MH (1954) A new review of the chlorites. Min Mag 30: 277–292.

Höll R (1975) Die Scheelitlagerstätte Felbertal und der Vergleich mit anderen Scheelitvorkommen in den Ostalpen. Bayerische Akademie der Wissenschaften, Math-naturwiss Klasse. Abh Neue Folge, Heft 157A

Hoernes S, Friedrichsen H (1974) Oxygen isotope studies on metamorphic rocks of the Western Hohe Tauern area (Austria). Schweiz Min Petr Mitt 54 (2–3): 769–788

Koller F, Richter W (1984) Die Metarodingite der Habachformation, Hohe Tauern (Österreich). Tschermaks Min Petr Mitt 33: 49–66

Leake BE ((1978) Nomenclature of amphiboles. Am Mineralogist 63: 1023–1052
Luckscheiter B, Morteani G (1980) Microthermometrical and chemical studies of fluid inclusions in minerals from alpine veins from the penninic rocks of the central and western Tauern Window (Austria/Italy). Lithos 13: 61–77
Morteani G (1974) Petrology of the Tauern Window, Austrian Alps, Excursion B9. Fortschr Min 52, Beiheft 1, Excursion Guidebook, pp 195–220
Satir M, Morteani G (1982) Petrological study and radiometric age determination of the migmatites in the penninic rocks of the Zillertaler Alpen (Tyrol/Austria). Tschermaks Min Petr Mitt 30: 59–75
Selverstone J, Spear F, Franz G, Morteani G (1984) High-pressure metamorphism in the SW Tauern Window, Austria: P-T paths from hornblende-kyanite-staurolite schists. J Petrol 25: 501–531
Sinkankas J (1981) Emerald and other beryls. Chilton Book Company, Radnor, Pennsylvania
Wood DL, Nassau K (1968) The characterization of beryl and emerald by visible and infrared absorption spectroscopy. Am Mineralogist 53: 777–800

Authors' addresses: Prof. G. Franz, Institut für Angewandte Geophysik, Petrologie und Lagerstättenforschung, Technische Universität Berlin, EB 310, Strasse des 17. Juni 135, D-1000 Berlin 12; Dr. G. Grundmann, Lehrstuhl für Angewandte Mineralogie und Geochemie, Technische Universität München, Lichtenbergstrasse 4, D-8046 Garching; Dr. D. Ackermand, Institut für Mineralogie der Universität Kiel, Olshausenstrasse 40–60, D-2300 Kiel, Federal Republic of Germany.